Journal of Science and Transport Technology
Journal homepage: https://jstt.vn/index.php/en

GIS Based Soil Erosion Susceptibility Assessment Using Deep Learning Models: A Case Study in the Mountainous Region of Nghe An, Vietnam

Giang Huong Pham[1], Bach Tuyet Thi Pham[2], Kieu Oanh Thi Hoang[2], Tuyen Thi Tran[2,*], Hoàng Nguyễn Đức Chí[3]

[1]Faculty of Geography, Thai Nguyen University of Education, Thai Nguyen University, Vietnam, giangph@tnue.edu.vn

[2]Faculty of Social sciences and Arts, Sai Gon University, Ho Chi Minh, Vietnam, bachtuyet@sgu.edu.vn, Htkoanh@sgu.edu.vn, tttuyen1982@sgu.edu.vn

[3]Geotechnical and Artificial Intelligence Research Group, University of Transport Technology, 54 Trieu Khuc, Thanh Liet, Hanoi 100000, Vietnam, chihnd@utt.edu.vn

Article info
Type of article:
Original research paper

DOI:
https://doi.org/10.58845/jstt.utt.2026.en.6.1.67-86

***Corresponding author:**
Email address:
tttuyen1982@sgu.edu.vn

Received: 12/10/2025
Received in Revised Form: 14/11/2025
Accepted: 02/12/2026

Abstract: In this study, the main objective is to evaluate soil erosion susceptibility in the mountainous region of Nghe An Province using three deep learning models: Long Short-Term Memory (LSTM), Deep Neural Network (DNN), and Deep Attention Network (DaNet). A total of 685 erosion points were identified from field surveys and satellite imagery, and nine spatial conditioning factors were used, including slope, aspect, curvature, elevation, rainfall, Normalized Difference Vegetation Index (NDVI), soil type, distance to faults, and geology. The dataset was split into 70% for training and 30% for validating. Various validation metrics including area under the ROC curve (AUC) were used for validation and comparison of the models. The results show that among the tested models, DaNet showed the highest predictive performance, achieving an AUC of 0.936 on the training dataset and 0.852 on the validating dataset compared with other deep learning models (DNN and LSTM). The susceptibility map produced by DaNet demonstrated strong spatial alignment with real-world erosion occurrences, with 59.88% of observed erosion points located in the very high susceptibility class and 18.52% in the high class, totaling 78.4% of all erosion events. These results confirm DaNet's effectiveness in capturing complex spatial patterns and delivering reliable erosion risk predictions, supporting its use for land-use planning.

Keywords: Soil Erosion, Deep Learning, Deep Attention Network, GIS, Vietnam.

1. Introduction

Soil erosion is one of the main causes of land degradation on a global scale, directly affecting food security, crop productivity, and ecosystem stability. Each year, the world loses approximately 12–15 tons of soil per hectare, equivalent to 0.9–0.95 mm of topsoil, due to erosion [1]. Among the various types, water-induced soil erosion is the most common and complex form, occurring through a sequence of processes over space and

time. It begins with rain splash erosion, where soil particles are detached from the surface due to the mechanical impact of raindrops and subsequently transported by surface runoff. As runoff becomes more concentrated, rill erosion develops, which can then evolve into gully erosion, causing substantial topsoil loss and altering the natural terrain [2]. The consequences go beyond just soil loss and include nutrient depletion, sedimentation, increased occurrence of mudflows, and the deterioration of soil ecological functions. Steep-slope regions, particularly in mountainous and humid tropical areas, are more severely affected due to the combination of several adverse factors such as high seasonal rainfall, rugged topography, reduced vegetation cover, and unsustainable land use practices.

Soil erosion results from the complex interaction between natural and anthropogenic factors [3]. On the natural side, key determinants include slope gradient, soil type, rainfall intensity, vegetation cover, and watershed morphology. Meanwhile, human induced activities such as deforestation, slash and burn agriculture, unsustainable farming on sloped land, and unplanned road construction have severely damaged the soil surface, reducing its protective and moisture-retention capabilities, thereby accelerating erosion rates many times higher than under natural conditions. Particularly in the context of climate change, the increasing frequency and intensity of extreme rainfall events have made even previously less vulnerable areas more erosion prone. This highlights the urgent need for accurate assessment of erosion susceptibility to support sustainable land use planning and the design of effective erosion control strategies.

Numerous studies around the world have been conducted to assess soil erosion using various methods, in which empirical models such as USLE and its improved version RUSLE have been the main tools for evaluating erosion at watershed or national scales due to their simplicity, low data input requirements, and ease of implementation [4]. However, the inherent limitations of these models lie in their empirical nature and simplification. Specifically, they assume linear relationships among erosion factors, produce long-term average results, and are unable to simulate temporal dynamics nor can they accurately reflect the spatial variability of the erosion process. To overcome these drawbacks, mathematical and physically based models have been developed to more precisely describe the sequence of erosion processes: rainfall, runoff, soil detachment, sediment transport, and deposition. Such models are capable of providing detailed spatial and temporal information, allowing for evaluation of the impacts of individual rainfall events or specific land management practices on erosion. However, their disadvantages include the need for large volumes of high-quality input data (e.g., high-resolution topographic maps, real-time rainfall data, and detailed physical and chemical soil properties), as well as the calibration of many empirical parameters [5]. In addition, their high computational cost and complex simulation procedures make them difficult to apply on a large scale, and they are generally only suitable for in-depth studies or small watershed applications where sufficient data and resources are available.

Recently, artificial intelligence methods such as machine learning and deep learning have been proven to be effective tools for predicting and mapping soil erosion susceptibility [6]. Unlike traditional physical or empirical models with fixed formulas, machine learning techniques allow models to be trained directly from observed data on erosion and influencing factors. Many studies have shown that machine learning models achieve high accuracy in assessing soil erosion susceptibility, and in many cases, even outperform classical models. Specifically, algorithms such as Random Forest (RF) [7], Support Vector Machine (SVM) [8], Artificial Neural Networks (ANN) [9], Decision Trees [10] and Ensemble methods (AdaBoost, Gradient Boosting, ...) [11] have been successfully applied to build soil erosion susceptibility maps in

many parts of the world. Garosi et al. (2019) applied RF, SVM, Naive Bayes (NB) and GAM models to predict rill erosion, and stated that RF model outperformed the others for rill erosion susceptibility modeling [12]. Ikram et al. (2025) integrated intelligent optimization algorithms such as Biogeography-Based Optimization (BBO), Salp Swarm Algorithm (SSA), and Whale Optimization Algorithm (WOA) with artificial neural network (ANN) models to predict soil erosion susceptibility, and proven that the SOS-MLP model achieved the highest performance compared with other models such as BBO-MLP and WOA-MLP [13]. In addition to traditional machine learning, deep learning algorithms such as Convolutional Neural Networks (CNN) [14], Recurrent Neural Networks (RNN) [15] and Long Short-Term Memory (LSTM) [15] have also been applied in soil erosion susceptibility studies. For instance, Khosravi et al. (2023) conducted one of the first studies to quantify the potential of deep learning models in erosion susceptibility mapping including CNN, RNN and LSTM models at a watershed in Iran, and the results showed that all three models performed very well, with the RNN model achieving higher accuracy than both CNN and LSTM [2].

In Vietnam, the application of deep learning techniques in soil erosion research has only begun in recent years [16]. Most previous studies focused on empirical methods or initially experimented with some traditional machine learning models; the number of studies applying deep neural networks combined with SHAP interpretation methods in soil erosion assessment remains very limited [17]. Therefore, the main objective of this study is to investigate and compare three deep learning models including LSTM, DNN, and Deep Attention Network (DaNet) for soil erosion susceptibility modeling and mapping in the mountainous area of Nghe An, Vietnam. Various validation indicators including area under the ROC curve (AUC) were used for validation and comparison of the models. In addition, SHapley Additive exPlanations (SHAP) and Local Interpretable Model-Agnostic Explanations (LIME) analysis were also used for interpretation of the model's performance.

2. Methods used

2.1. Deep Attention Network (DaNet)

DaNet is a deep learning architecture that integrates attention mechanisms into conventional neural network structures to enhance feature representation and model interpretability [18]. Its core principle relies on dynamically assigning weights to different parts of the input data, allowing the network to focus selectively on the most informative features while suppressing irrelevant or redundant information. Typically, attention layers are incorporated into convolutional or recurrent frameworks, enabling the model to capture both local and global dependencies more effectively. By guiding the learning process toward critical spatial or temporal regions, DaNet improves both prediction accuracy and robustness across diverse tasks [19]. This makes it particularly well-suited for applications involving heterogeneous input data, such as environmental modeling, image analysis, and sequential forecasting, where understanding the contextual importance of input variables is essential.

2.2. Deep Neural Network (DNN)

DNN operates based on the principle of nonlinear function approximation through multiple fully connected layers [20]. The model transforms input data into progressively abstract representations using nonlinear activation functions, while weight optimization is performed through backpropagation. Over iterative training, the network learns implicit relationships between input and output variables without relying on predefined spatial or sequential structure. DNNs are typically applied when the objective is to capture complex underlying relationships in aggregated datasets where the data do not inherently exhibit ordered or spatial relationships [21].

2.3. Long Short-Term Memory (LSTM)

LSTM represents a deep recurrent architecture developed to model sequential data or

information with temporal dependencies [22]. It employs a gated structure consisting of an input gate, forget gate, and output gate to regulate the flow of information during training. This mechanism allows the model to selectively store, update, or discard information over time, enabling the retention of long-range dependencies while mitigating vanishing or exploding gradients often encountered in traditional recurrent neural networks [23]. As a result, LSTM is appropriate for learning dynamic patterns where sequence continuity and temporal context are critical to model representation.

2.4. Validation methods

2.4.1. Receiver operating characteristic curve (ROC)

ROC curve is employed as an evaluation tool to assess the classification capability of the developed models [24-26]. This graphical representation illustrates the relationship between the True Positive Rate (TP) and the False Positive Rate (FP) across a range of classification thresholds, thereby demonstrating how effectively the model can distinguish between the two data classes. The metric associated with the ROC curve is the Area Under the Curve (AUC), which serves as a comprehensive indicator of classification performance: a value approaching 1 reflects strong separability between classes, whereas a value near 0.5 indicates that the model performs at a level similar to random classification [27]. Values of AUC can be calculated by following equation:

$$AUC = \frac{\left(\sum TP + \sum TN\right)}{\left(P + N\right)} \quad (1)$$

where, TP is the number of Soil erosions that is correctly classified, TN is the number of incorrectly classified Soil erosions, P is the total number of Soil erosions and N is the total number of non-Soil erosions.

2.4.2. Statistical Indexes

Other statistical indicators used for model assessment include Positive Predictive Value (PPV), Negative Predictive Value (NPV), sensitivity (SST), specificity (SPF), accuracy (ACC), Cohen's Kappa coefficient (K), Root Mean Square Error (RMSE), and Mean Absolute Error (MAE) [28, 29]. Among these, the Kappa coefficient measures the level of agreement beyond random chance, with values ranging from 0 to 1. A value closer to 1 indicates higher reliability and stronger agreement between predicted and observed classifications, whereas values approaching 0 suggest weak or random agreement. RMSE represents the squared deviation between observed and predicted values, while MAE measures the average magnitude of the prediction error regardless of direction [30, 31]. A model is considered to perform well when the statistical indicators such as SPF, PPV, NPV, ACC, SST, and K demonstrate high values, while error-based metrics including RMSE and MAE show decreasing trends [32-35].

2.5. SHapley Additive exPlanations (SHAP) analysis

SHAP method was applied to interpret the contribution of each input variable to the model's prediction results. SHAP is grounded in cooperative game theory, where each variable is conceptualized as an independent "player" contributing to the final prediction generated by the model [36]. Through the computation of Shapley values, the method quantifies the marginal contribution of each variable by comparing model outputs across all possible combinations of feature subsets. This theoretical framework ensures fairness in attribution and provides an objective measure of how individual variables influence predictive behavior.

Importantly, SHAP facilitates interpretability at multiple analytical levels. At the global level, SHAP identifies variables that consistently exert the greatest influence across the entire dataset and reveals broader patterns of feature impact. At the local level, the method enables examination of how specific variables affect individual predictions, thereby allowing the interpretation of case-specific reasoning within the model. This dual capability is particularly valuable when working with complex

deep learning approaches, which are often characterized as “black-box” models. By enhancing transparency and explanatory depth, SHAP provides a foundation for model validation, supports decision-making processes, and increases trustworthiness in model outputs, especially in applications where interpretability and reliability are essential [37].

2.6. Local Interpretable Model-Agnostic Explanations (LIME) analysis

Local Interpretable Model-Agnostic Explanations (LIME) is a post-hoc interpretability technique designed to explain the predictions of any black-box machine learning model [38]. It operates under the principle that while complex models may be difficult to interpret globally, their behavior can be approximated locally around a specific prediction using a simpler, interpretable model (such as linear regression or decision trees).

LIME works by perturbing the input data around the instance of interest and observing how these perturbations affect the model’s predictions [39]. It then assigns weights to the perturbed samples based on their similarity to the original instance and fits a local surrogate model to approximate the complex model’s decision boundary in the neighborhood of the instance. The resulting explanation highlights which features contributed most positively or negatively to the model’s output for that particular case.

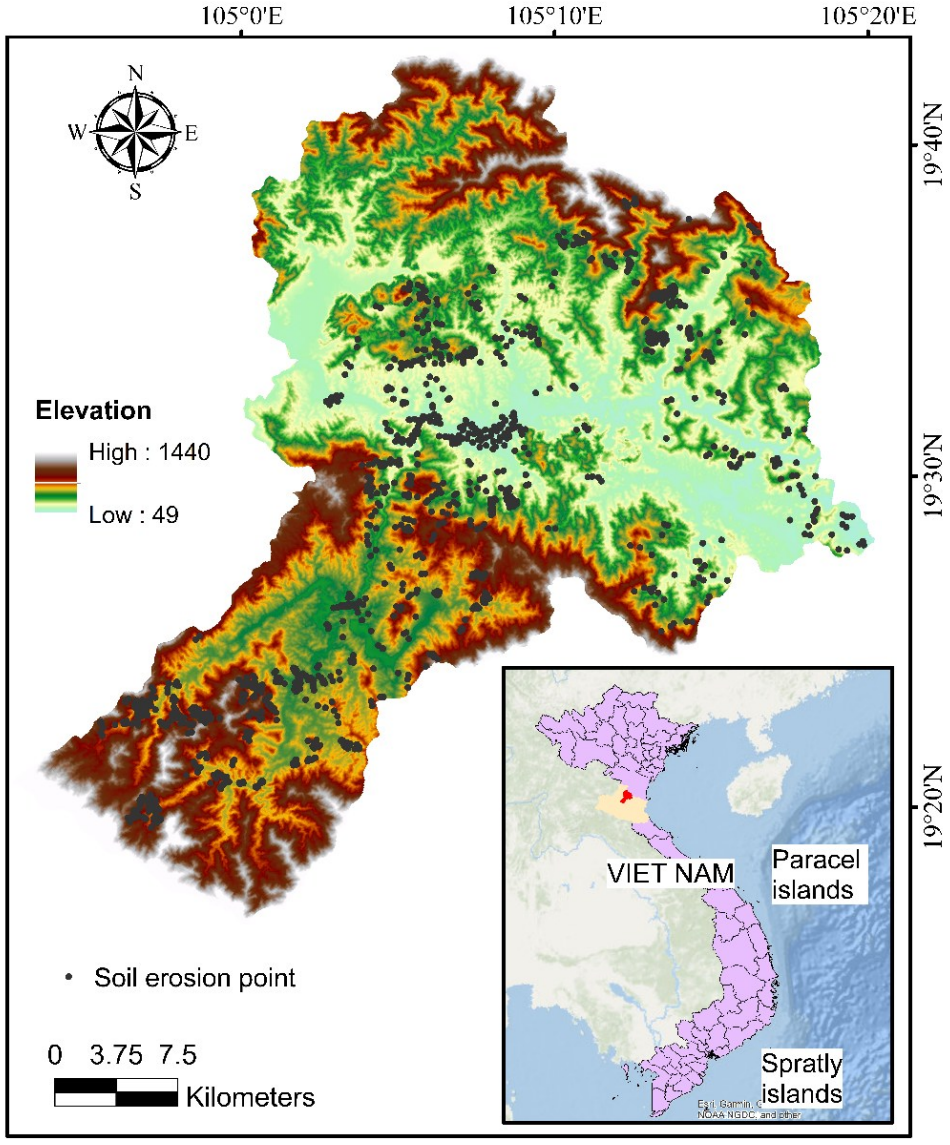

Fig. 1. Location of the study area and historical Soil erosions

3. Study area

The study area is located in Nghe An Province, belonging to the middle and upper parts of the Lam River basin, with a total area of approximately 1,074 km² (Fig 1). The topography varies significantly from west to east, where the western region is influenced by the Truong Son mountain system and is characterized by high mountains and steep hillslopes, while the eastern part mainly consists of low-lying coastal plains. Elevation ranges from about 50 m to more than 1,500 m above sea level, with some areas having slopes greater than 35°, which creates favorable conditions for surface erosion and mass movement processes. In terms of geological characteristics, Nghe An contains a complex lithological structure with the distribution of various metamorphic and sedimentary rocks. In many locations, the soil layer is thin, highly mineralized, and easily weathered under tropical climatic conditions, leading to considerable spatial variability in soil erodibility. The climate in the region is classified as tropical monsoon with two distinctly defined seasons: a dry season extending from November to April and a rainy season occurring from May to October. The average annual rainfall ranges between 1,600 and 1,800 mm; however, during years affected by strong typhoons, rainfall may exceed 2,500 mm. Short-duration heavy rainfall events, especially during the storm period, typically generate strong surface runoff and act as a primary agent triggering erosion.

Soil erosion in the study area results from a combination of multiple driving factors. Natural conditions such as steep topography, concentrated seasonal rainfall, reduced vegetation cover, and highly weathered soils play a significant role in accelerating erosion. Meanwhile, anthropogenic activities, including deforestation, agricultural expansion on sloping terrain, slash and burn cultivation, mining operations, and unsustainable farming practices, have intensified soil degradation and increased erosion risk. In addition, the growing influence of climate change, particularly the increasing frequency and intensity of extreme rainfall events, is contributing to more severe and widespread erosion processes across the region.

4. Data used

4.1. Landside inventory

Soil erosion inventory dataset comprises 685 erosion points identified within the Lam River basin located in Nghe An Province [40]. The locations were determined through an integrated approach combining multiple sources, including Google Earth satellite image interpretation, consultation of local reports and documentation, remote sensing data analysis, and field verification surveys. During fieldwork, a GPS device was used to precisely record the coordinates of each erosion point in order to ensure spatial accuracy and data reliability [41]. This combined approach helps minimize spatial uncertainty while providing a comprehensive representation of the actual soil erosion conditions within the study area.

4.2. Soil erosion influencing factors

A total of ten input factors used in the model were compiled from multiple geospatial data sources, including topographic data, climatic information, vegetation cover, and geological pedological characteristics (Table 1). All datasets were preprocessed, standardized, and projected into a unified spatial reference system to ensure compatibility and consistency throughout the analytical workflow. The datasets were then converted into raster format with a spatial resolution of 30 × 30 m using ArcGIS 10.8. Data classification was performed using either the Natural Breaks method or logical grouping, depending on the characteristics of each variable, to accurately represent the natural distribution and spatial variability of conditions across the study area [40, 42].

Elevation is a controlling factor influencing soil erosion processes. As elevation increases, shifts in micro-climatic conditions may reduce vegetation density and enhance rock and soil fragmentation, which creates favorable conditions for erosion [43]. Additionally, areas with medium to

high elevation are typically characterized by strong terrain dissection, resulting in steeper slopes and more concentrated surface runoff compared to lower plain regions. In this study, the elevation layer was classified into 6 categories using the Natural Breaks method: 203–336 m, 336–474 m, 474–629 m, 629–829 m và 829–1440 m (Fig 2.a).

Aspect is an important topographic variable influencing surface micro-environmental conditions. South, Southwest and West facing slopes experience prolonged solar exposure, resulting in higher temperatures, faster evaporation, and lower soil moisture [44]. These conditions often lead to reduced vegetation cover and decreased soil protection against rainfall and runoff, thereby increasing erosion susceptibility. In contrast, North- and Northeast-facing slopes are generally cooler and wetter, allowing denser vegetation growth and reduced soil erosion. In this study, aspect was classified into 9 classes: Flat, North, Northeast, East, Southeast, South, Southwest, West, and Northwest (Fig 2.b).

Table 1. Input factors influencing soil erosion considered for the study area [40]

No.	Influencing factor	Resolution/Scale	Data source
1	Elevation	30 m	Digital Elevation Model (DEM) – USGS
2	Aspect	30 m	Derived from DEM
3	Slope	30 m	Derived from DEM
4	Curvature	30 m	Derived from DEM
5	NDVI	30 m	Landsat 8 imagery
6	Land cover	1:200,000	Ministry of Agriculture and Environment
7	Rainfall	-	Vietnam Meteorological and Hydrological Administration
8	Distance to faults	1:200,000	Department of Geology and Minerals of Vietnam
9	Geology	1:200,000	Department of Geology and Minerals of Vietnam

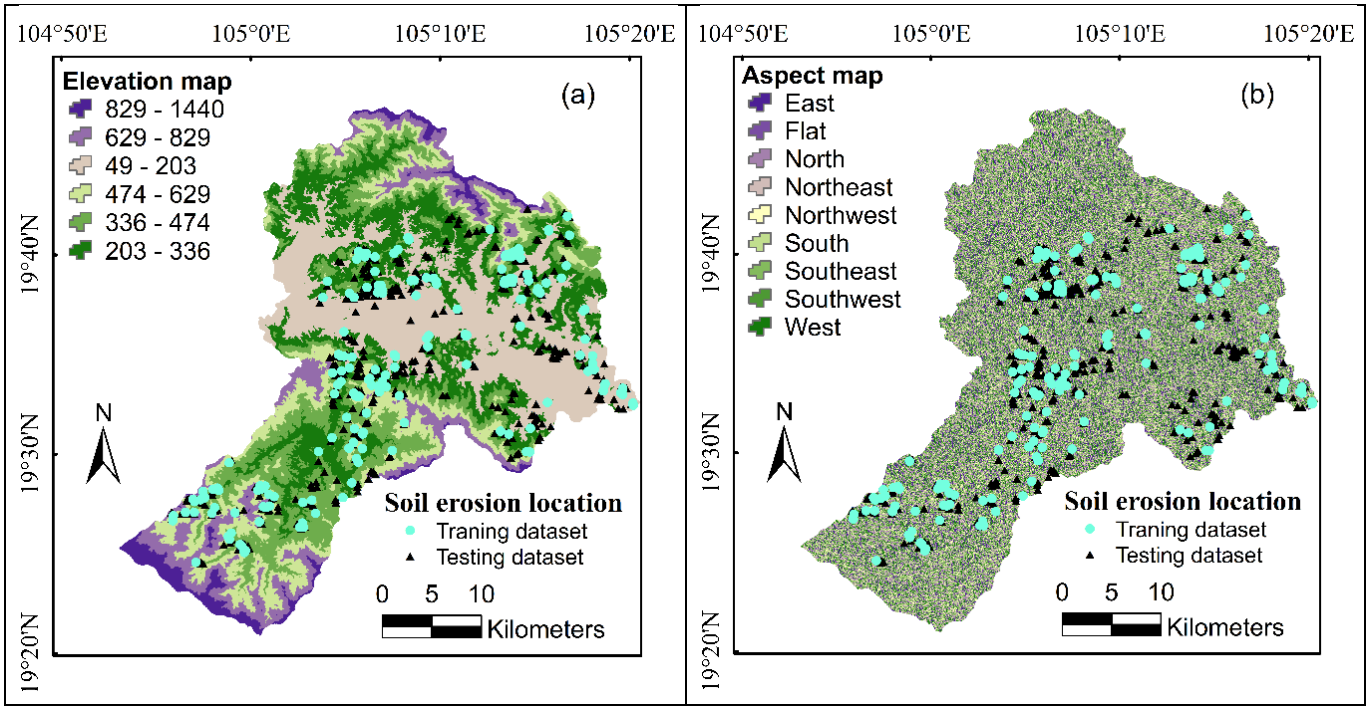

Fig. 2. Thematic maps of the study area: (a) Elevation; (b) Aspect; (c) Slope; (d) Curvature; (e) NDVI; (f) Soil type; (g) Rainfall; (h) Distance to faults; (i) Geology [40]

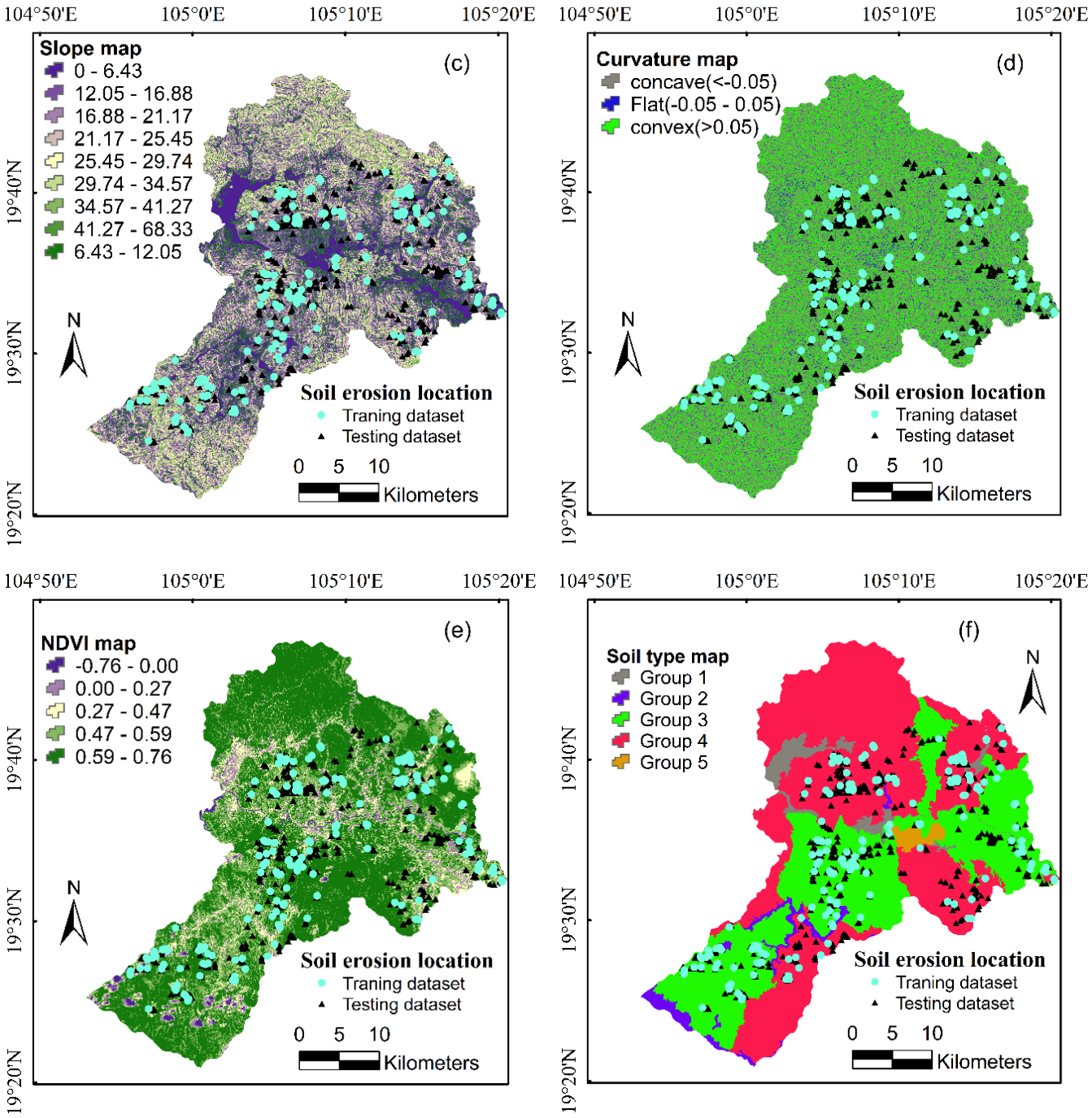

Fig. 2. (continued)

Slope exerts direct control over gravitational forces and runoff velocity. As slope increases, the infiltration capacity of soil decreases due to shorter water contact time, which leads to an increase in surface runoff [45]. This process reduces surface stability and increases the likelihood of soil detachment. The slope layer was classified into 9 classes: 0–6.43°, 6.43–12.05°, 12.05–16.88°, 16.88–21.17°, 21.17–25.45°, 25.45–29.74°, 29.74–34.57°, 34.57–41.27°, và 41.27–68.33° (Fig 2.c).

Curvature represents surface morphology and reflects the potential for surface flow convergence or divergence. Concave surfaces tend to accumulate water, facilitating the development of rill erosion or small-scale mass movement, whereas convex surfaces disperse runoff, reducing concentrated flow energy and erosion potential [46]. The curvature values were divided into 3 groups: < –0.05 (concave), –0.05 to

0.05 (flat), and > 0.05 (convex) (Fig 2.d).

Normalized Difference Vegetation Index (NDVI) represents vegetation cover, which acts as a natural barrier to erosion by reducing raindrop impact, increasing water infiltration, and stabilizing soil structure through root systems [47]. Low NDVI values indicate exposed soil, cultivated agricultural land, or disturbed vegetation due to logging or wildfires, which leads to increased runoff and accelerated erosion. NDVI in this study was classified into 5 groups using the Natural Breaks method: -0.76–0.00, 0.00–0.27, 0.27–0.47, 0.47–0.59, 0.59–0.76 (Fig 2.e).

Soil type represents physical and mechanical properties including grain size distribution, porosity, permeability, cohesion, bulk density, and moisture retention all of which directly influence surface resistance to erosion [48]. Coarse textured, weakly cohesive, or highly weathered soils are more susceptible to erosion under high rainfall or steep slope conditions, while clay rich soils with well-developed vegetation cover generally have higher structural resistance. In this study, the soil type layer was classified into 5 groups: Red-yellow ferralite soil formed on sandstone, Red-yellow ferralite formed on acidic igneous rocks, Red-yellow soil is formed on metamorphic rocks, Humus on the mountain, Alluvial soil in the valley soil (Fig 2.f).

Rainfall is the primary triggering factor of erosion through two dominant mechanisms: (i) raindrop impact, which disrupts soil aggregates, and (ii) increased runoff following soil saturation, which leads to surface wash, rill erosion, and sediment transport [49]. Rainfall values were classified into 4 groups using the Natural Breaks method: 20 mm, 20–40 mm, 40–80 mm và >80 mm (Fig 2.g).

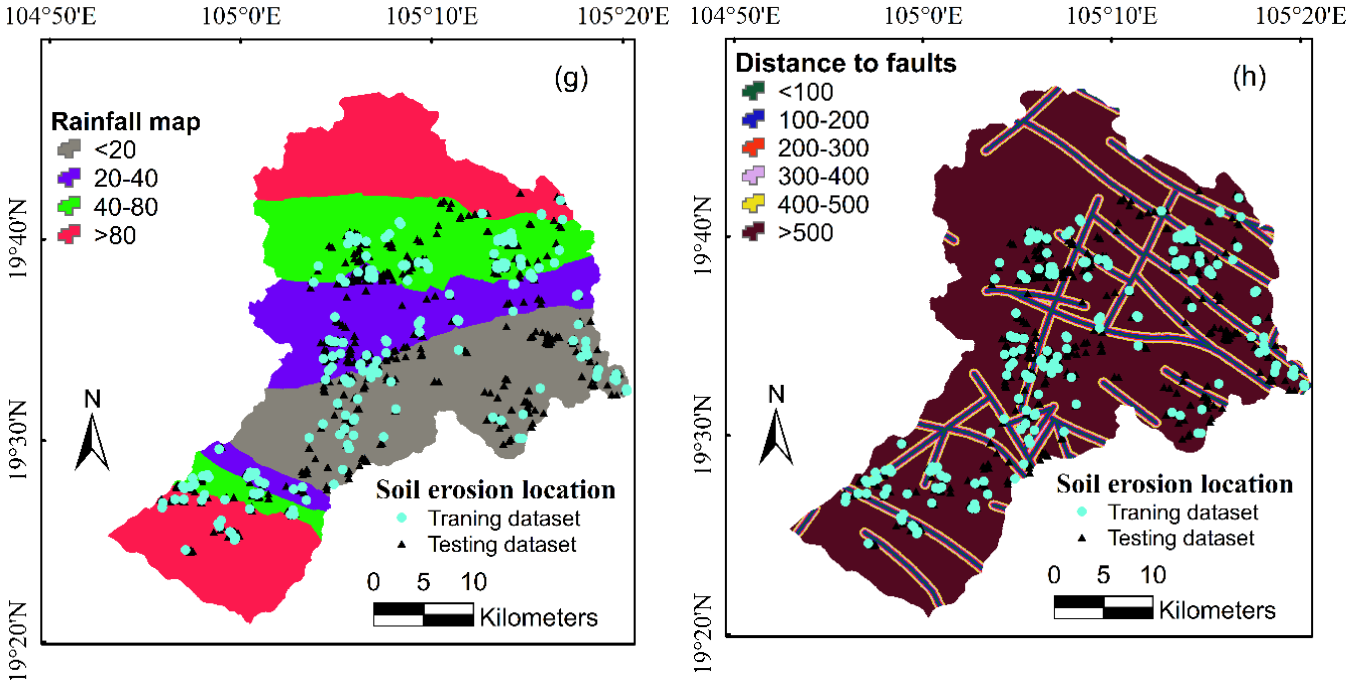

Fig. 2. (continued)

Distance to faults map plays a critical role in analyzing soil erosion susceptibility, as geological faults can weaken the soil structure, facilitate rainwater infiltration, concentrate surface runoff, and thereby accelerate erosion processes [50]. Areas located near fault zones are often more vulnerable to geological and hydrological disturbances, leading to ground surface instability and an increased risk of topsoil removal. This map illustrates the spatial distribution of regions located at varying distances from geological fault lines within the study area. The data are classified into six categories: <100 m, 100–200 m, 200–300 m, 300–400 m, 400–500 m, >500 m, consistent with

the legend shown in the figure (Fig 2.h).

Geological plays a fundamental role in determining weathering processes, soil material composition, and slope stability. Weak or highly weathered formations tend to produce loose materials that are easily detached, whereas magmatic or metamorphic formations with higher structural strength are less susceptible to erosion [51]. In this study, geology was classified into 17 groups: Dai Loc Complex Phase 1, Bac Son Formation, Bu Khang Formation Upper Subformation, Dai Loc Complex Phase 2, Dong Do Formation Lower Subformation, Dong Trau Formation Lower Subformation, Dong Trau Formation Upper Subformation, Huoi Loi Formation, Huoi Nhi Formation, La Khe Formation, Muong Hing Formation, Nam Kan Formation, Song Ca Formation Lower Subformation, Song Ca Formation Middle Subformation, Song Ca Formation Upper Subformation, Song Ma Complex, and Undivided Quaternary (Fig 2.i).

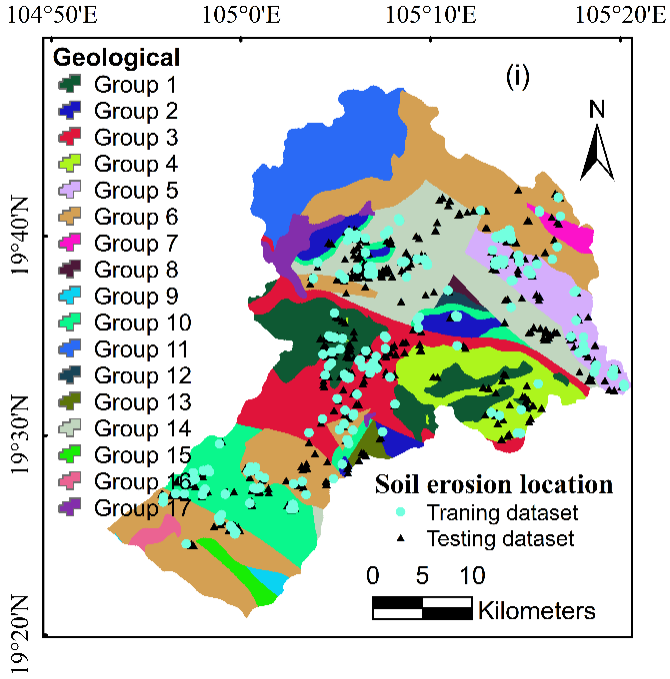

Fig. 2. (continued)

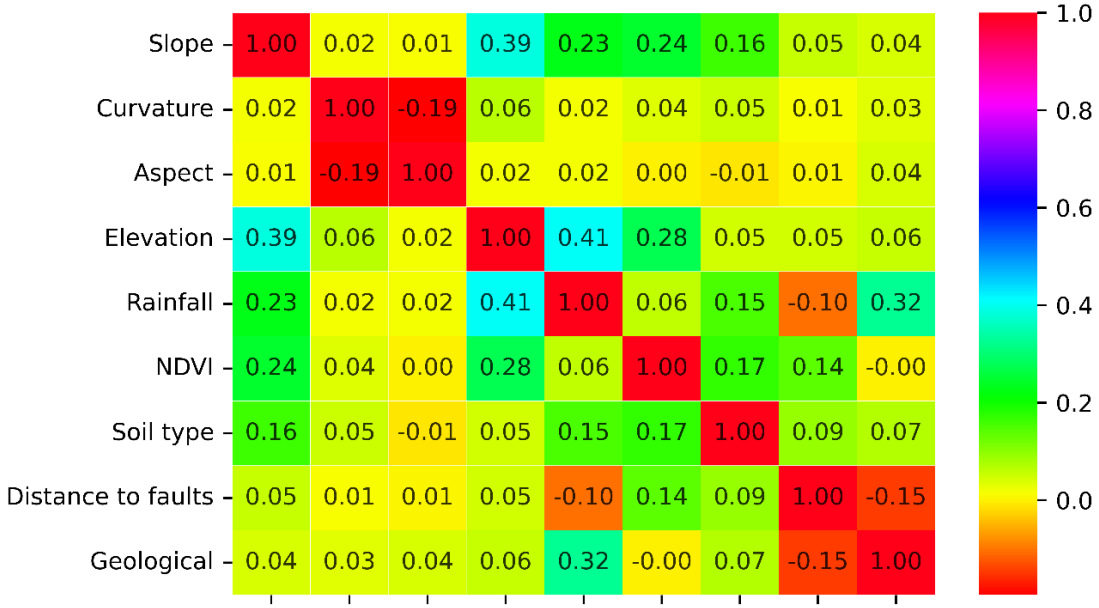

Fig. 3. Correlation matrix of the input variables

The correlation among input variables in the model was examined using the pearson correlation coefficient [52]. As shown in Fig. 3, most variables exhibit low to moderate correlation levels. The color gradient in the heatmap represents the strength of correlations, where lighter colors indicate stronger positive relationships, and darker colors represent weaker or negative ones. Overall, the low inter-variable correlations suggest minimal multicollinearity, indicating that the dataset is suitable for model development without the need to eliminate any variables.

5. Results and discussion

5.1. Validation and comparison of the models

Evaluation metrics on the training dataset reveal notable differences in model performance across the tested algorithms (Table 2). Among them, the DaNet model demonstrates superior classification capability. It achieved the highest overall accuracy (ACC = 85.71%) and Cohen's Kappa value (0.715), indicating strong agreement between predicted and actual classes beyond random chance. Regarding error measures, DaNet attained the lowest mean absolute error (MAE = 0.143) and root mean square error (RMSE = 0.378), outperforming DNN (MAE = 0.176; RMSE = 0.420) and LSTM (MAE = 0.198; RMSE = 0.445). In classification counts, DaNet obtained the highest number of true positives (TP = 403) and true negatives (TN = 419), along with the lowest number of false positives (FP = 53) and a relatively low number of false negatives (FN = 84). Additionally, DaNet scored highest in PPV (88.38%), NPV (83.30%), and SPF (88.77%), confirming its robustness, precision, and strong predictive performance during training.

Table 2. Validation and comparison of the models

No	Parameters	Training dataset			Validating dataset		
		DaNet	DNN	LSTM	DaNet	DNN	LSTM
1	TP	403	375	376	152	139	135
2	TN	419	415	393	168	181	171
3	FP	53	57	79	45	32	42
4	FN	84	112	111	46	59	63
5	PPV (%)	88.38	86.81	82.64	77.16	81.29	76.27
6	NPV (%)	83.3	78.75	77.98	78.5	75.42	73.08
7	SST (%)	82.75	77	77.21	76.77	70.2	68.18
8	SPF (%)	88.77	87.92	83.26	78.87	84.98	80.28
9	ACC (%)	85.71	82.38	80.19	77.86	77.86	74.45
10	Kappa	0.715	0.648	0.604	0.557	0.554	0.486
11	MAE	0.143	0.176	0.198	0.221	0.221	0.255
12	RMSE	0.378	0.42	0.445	0.471	0.471	0.505

Validating results follow a similar trend, reinforcing the generalization capability of the models. DaNet continued to outperform other models with the highest number of true positives (TP = 152), the lowest number of false negatives (FN = 46), and competitive true negative and false positive values (TN = 168; FP = 45). The overall accuracy reached 77.86%, higher than DNN and LSTM (77.86% and 74.45%, respectively), while maintaining the highest Cohen's Kappa value (0.557). DaNet also delivered low error rates (MAE = 0.221; RMSE = 0.471), comparable to the other models and better than LSTM. Supporting metrics such as PPV (77.16%), NPV (78.50%), and SST (76.77%) further validate its consistent and reliable performance on unseen data. Overall, these results confirm that DaNet is the most effective and reliable model among those tested, offering strong

classification accuracy, minimal error, and high generalization ability for soil erosion susceptibility mapping.

Based on the ROC analysis shown in Fig. 4, model performance was evaluated on both the training and validating datasets. On the training dataset, the DaNet model achieved the highest AUC value (0.936), followed by DNN (0.912) and LSTM (0.891), indicating DaNet's superior classification capability during the learning phase. The validating results reaffirm this trend, with DaNet maintaining top performance at an AUC of 0.852, followed by DNN (0.843) and LSTM (0.816). All models demonstrated reasonably high predictive accuracy, but DaNet stood out in terms of generalization and stability when applied to unseen data. Overall, DaNet proved to be the most effective model across both datasets, thanks to its strong feature learning capacity and low prediction error. This makes it particularly well-suited for soil erosion prediction and susceptibility mapping at practical application scales.

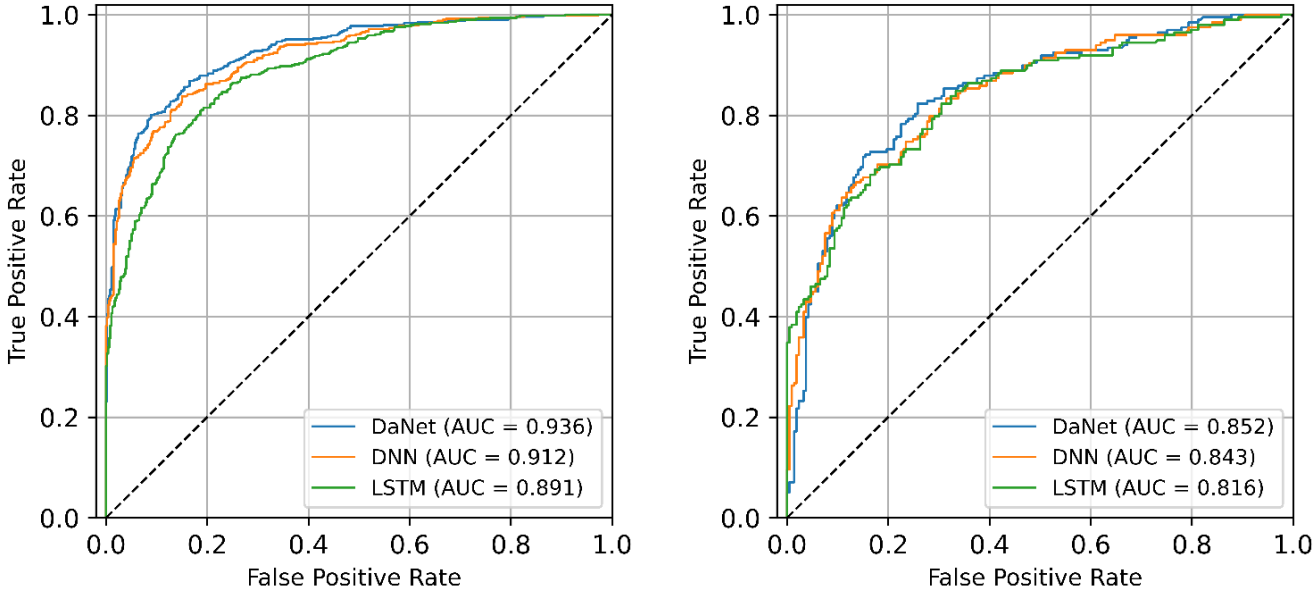

Fig. 4. AUC analysis of the models using (a) training dataset and (b) validating dataset

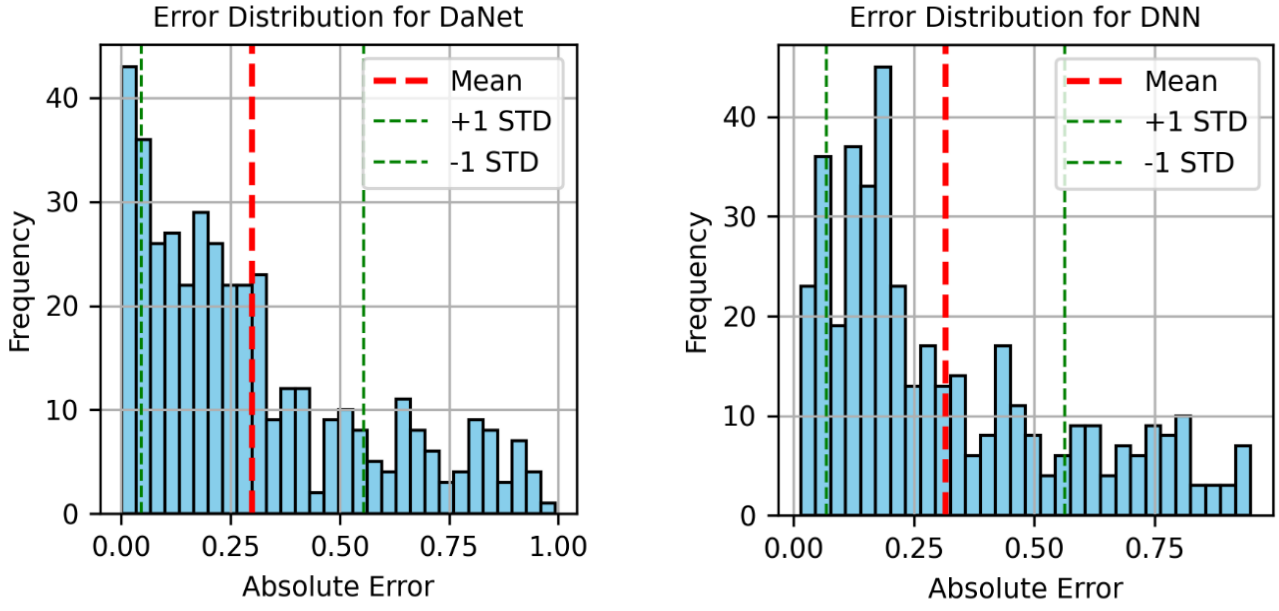

Fig. 5. Error distribution analysis: (a): DaNet; (b): DNN; (c): LSTM models

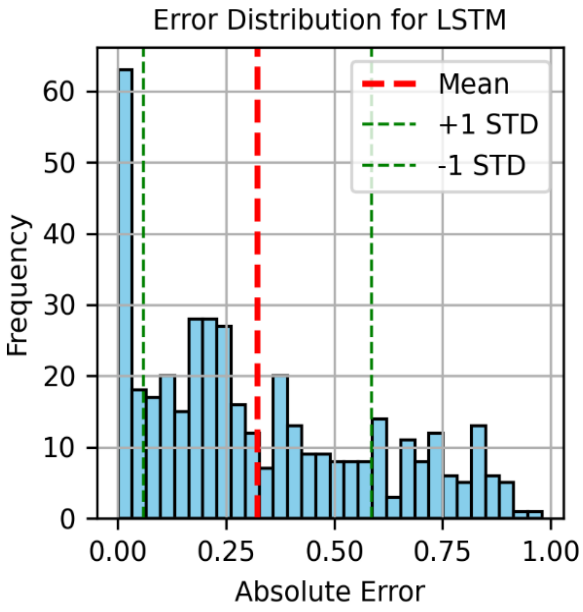

Fig. 5. (continued)

The error distribution analysis for the DaNet, DNN, and LSTM models provides valuable insights into the stability and reliability of each model's predictions (Fig. 5). Among the three, DaNet shows the most concentrated distribution around low absolute error values, with a sharp peak near zero and narrow bounds within ±1 standard deviation. This indicates that DaNet consistently produces accurate predictions with minimal variability. In comparison, the DNN model maintains a peak at lower error values but still displays moderate dispersion, suggesting some variability in performance. The LSTM model, while having a notable number of predictions with low errors, demonstrates the widest spread, including many higher-error cases up to 0.9. This indicates less consistent performance and a higher susceptibility to misprediction compared to DaNet and DNN.

In general, the results of validation and comparison of the models proven that the proposed DaNet model provides a clear improvement in predictive performance for susceptibility mapping compared with the benchmark DNN and LSTM models. Compared with the previously published study [40] which applied advanced machine-learning approaches to the same study area using different model structures, several important distinctions emerge. While the earlier study reported strong predictive performance using ensemble and tree-based learning methods, the present results show that a deep learning architecture such as DaNet can achieve comparable or improved generalization performance, particularly in terms of balanced ACC (77.86% for DaNet compared with 74.209% for Gradien Boosting) and validation AUC (0.852 for DaNet compared with 0.83 for Gradien Boosting) [40]. Unlike ensemble methods that rely on aggregating multiple weak learners or rule-based inference, the DaNet directly learns hierarchical feature representations from the input data, enabling it to model complex nonlinear interactions more efficiently. Moreover, the reduced prediction error and stable validation behavior observed in this study suggest that deep learning offers a competitive and scalable alternative for susceptibility mapping, especially when high-dimensional and correlated environmental variables are involved. Overall, the comparison indicates that the DaNet framework not only matches but in some aspects surpasses previously published models for this region, reinforcing the growing potential of deep learning approaches for geospatial hazard prediction.

5.2. Sensitivity analysis using SHAP and LIME analysis

The SHAP summary plot reveals the relative importance of input variables in the soil erosion prediction model based on their mean absolute SHAP values. Among the evaluated factors, soil type emerges as the most influential variable (+0.12), followed closely by geological characteristics (+0.10), and both slope and elevation (each at +0.06). These findings highlight the dominant role of soil properties, subsurface lithology, and terrain morphology in determining erosion susceptibility. Rainfall and aspect show moderate influence (+0.05), reflecting their involvement in runoff processes and slope orientation effects. In contrast, variables such as distance to faults and NDVI (both at +0.03), along with curvature (+0.02), contribute less significantly, suggesting a relatively lower but still notable impact on erosion potential compared to the leading geomorphological and geological predictors (Fig 6).

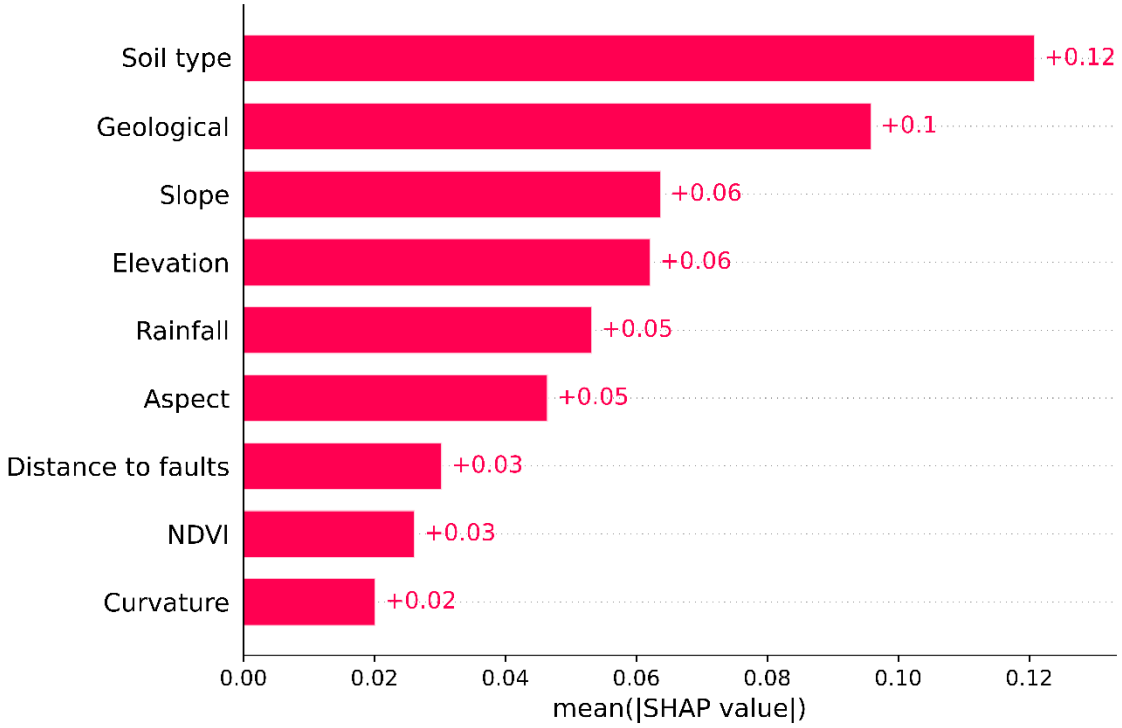

Fig. 6. Mean absolute SHAP values indicating the relative contribution of each predictor variable to the DaNet soil erosion prediction model

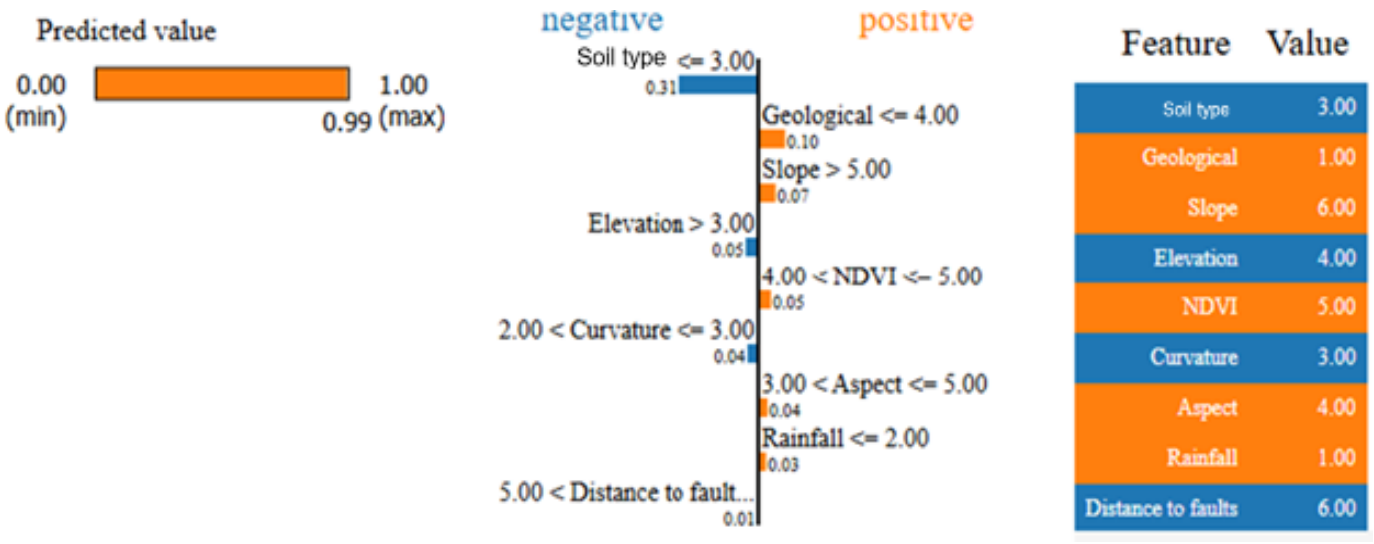

Fig. 7. Local interpretable model explanation (LIME) for sample ID47 using the DaNet model

The LIME analysis for sample 47 using the DaNet model reveals a very high soil erosion susceptibility score of 0.99 (Fig. 7). This prediction is primarily influenced by unfavorable geological conditions, which contribute significantly to the risk, along with steep slope, moderate elevation, and low vegetation cover (as indicated by NDVI). These factors suggest the area has weak geological stability, steep terrain, and sparse plant protection, all of which promote surface runoff and soil detachment. In contrast, land cover is the most influential factor reducing the erosion risk, indicating that current land use or vegetation may provide some degree of stabilization. Minor negative effects also come from terrain curvature and distance to fault lines. Overall, the model attributes high susceptibility mainly to geologic and topographic drivers, while land cover offers a key mitigating influence.

5.3. Construction of Soil erosion susceptibility maps

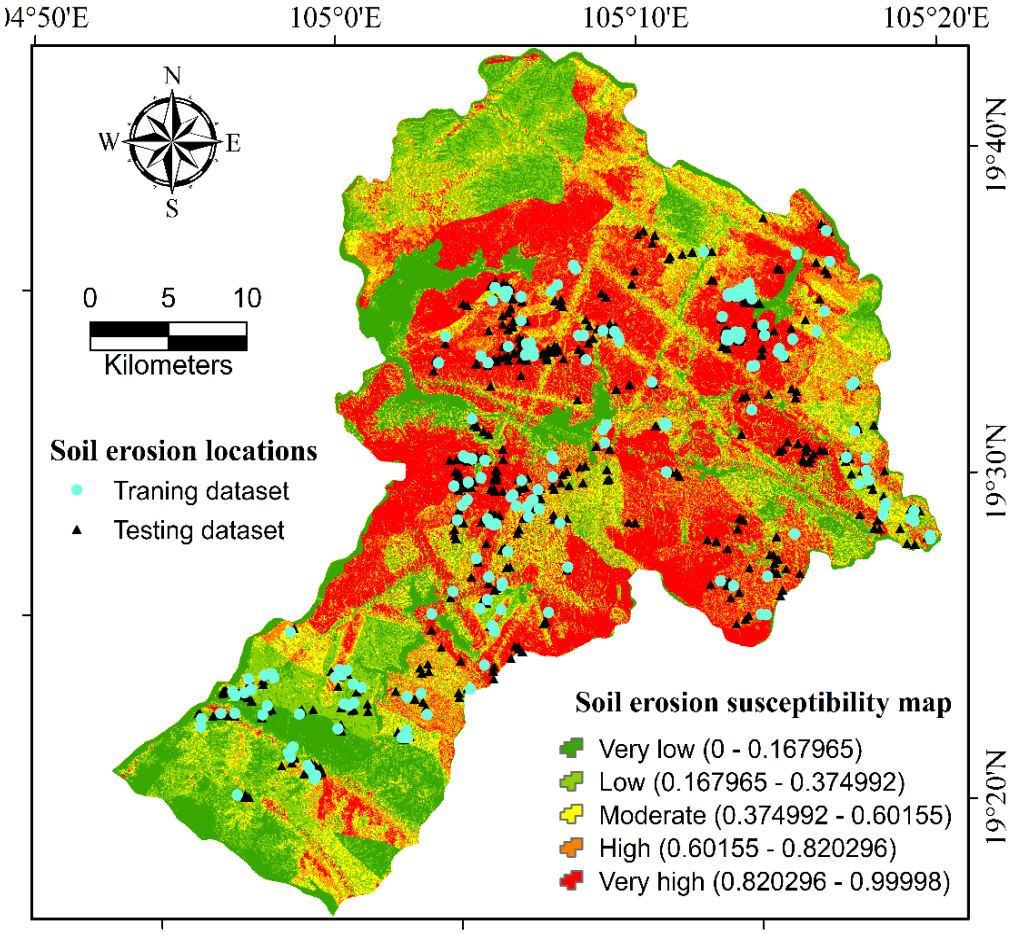

Fig. 8. Soil erosion susceptibility map using the DaNet model

Table 3. Analysis of spatial distribution of soil erosion susceptibility map generated by the DaNet model

No	Classes	FR	Percentage of class pixels (%)	Percentage of soil erosion pixels (%)
1	Very low (0.000 – 0.168)	0.099	18.66	1.85
2	Low (0.168 – 0.375)	0.534	17.34	9.26
3	Moderate (0.375 – 0.602)	0.691	15.18	10.49
4	High (0.602 – 0.820)	1.065	17.38	18.52
5	Very high (0.820 – 1.000)	1.905	31.44	59.88

The soil erosion susceptibility map was produced based on continuous prediction values generated by the best performance model of DaNet. Each pixel in the study area was assigned a value ranging from 0 to nearly 1, representing its susceptibility to soil erosion. These values reflect the relative likelihood of erosion occurrence, derived from spatial patterns learned during the training phase. The map uses a color gradient from dark green to red, where green indicates areas with very low erosion risk and red represents regions with very high susceptibility [53]. To facilitate interpretation, the continuous values were reclassified into 5 susceptibility classes using the Natural Breaks method: very low (0.000–0.168), low (0.168–0.375), moderate (0.375–0.602), high (0.602–0.820), and very high (0.820–1.000). This classification enhances visual clarity and helps distinguish spatial erosion risk levels effectively. Training and validating soil erosion locations are also overlaid on the map to validate model predictions and highlight areas of concern (Fig. 8).

The spatial distribution and predictive relevance of each soil erosion susceptibility class are clearly illustrated in Table 3. The frequency ratio (FR) steadily increases from the very low class (0.099) to the very high class (1.905), suggesting a strong positive relationship between predicted susceptibility levels and the actual occurrence of erosion. Areas classified as very high are nearly twice as likely to experience erosion compared to the average, while very low areas are significantly less prone. In terms of spatial coverage, the very high class comprises the largest proportion of the study area (31.44%) and contains the vast majority of observed erosion pixels (59.88%), confirming its predictive significance. Conversely, the very low class, while covering 18.66% of the land, accounts for only 1.85% of erosion points. The moderate and high classes serve as transitional zones, capturing increasing shares of erosion presence with moderate spatial coverage. These findings highlight the model's strong capacity to distinguish between erosion-prone and stable regions.

6. Concluding remarks

This study applied three deep learning models, DNN, LSTM and DaNet, to assess soil erosion susceptibility in the mountainous region of Nghe An Province. Various validation metrics including area under the ROC curve (AUC) were used for validation and comparison of the models. Results of this study show that the DaNet consistently outperformed the others, achieving the highest evaluation metrics with an AUC of 0.936 (training) and 0.852 (validating), along with solid classification accuracy (ACC = 0.857) and a substantial Kappa coefficient of 0.714. Error rates were also low (MAE = 0.143; RMSE = 0.378), highlighting the model's robustness and reliability. The susceptibility map generated by DaNet showed strong spatial alignment with observed erosion points, with 18.52% falling in the high-risk class and 59.88% in the very high-risk class, together accounting for 78.4% of all erosion events. These findings demonstrate that DaNet is the most effective model in this study, capable of capturing complex spatial patterns and providing accurate, stable predictions. It proves to be a promising tool for erosion monitoring, land-use planning and watershed management. Future work should explore the integration of multi-temporal data, climate variability scenarios and advanced optimization strategies to further improve the model.

Funding: This work is a part of the research project [CS.2025.A4.049] funded by Saigon University.

Conflict of Interest: The authors declare that there is no conflict of interest.

References

[1] R. Lal. (2020). Soil erosion and gaseous emissions. *Applied Sciences*, 10(8), 2784. https://doi.org/10.3390/app10082784

[2] K. Khosravi, F. Rezaie, J.R. Cooper, Z. Kalantari, S. Abolfathi, J. Hatamiafkoueieh. (2023). Soil water erosion susceptibility assessment using deep learning algorithms. *Journal of Hydrology*, 618, 129229.

https://doi.org/10.1016/j.jhydrol.2023.129229

[3] M.A. Nearing, Y. Xie, B. Liu, Y. Ye. (2017). Natural and anthropogenic rates of soil erosion. *International Soil and Water Conservation Research*, 5(2), 77-84. https://doi.org/10.1016/j.iswcr.2017.04.001

[4] A. Luvai, J. Obiero, C. Omuto. (2022). Soil loss assessment using the revised universal soil loss equation (RUSLE) model. *Applied and Environmental Soil Science*, 2022, 2122554. https://doi.org/10.1155/2022/2122554

[5] J. Wang, J. Yang, Z. Li, L. Ke, Q. Li, J. Fan, X. Wang. (2025). Research on soil erosion based on remote sensing technology: A review. *Agriculture*, 15(1), 18. https://doi.org/10.3390/agriculture15010018

[6] M. Biglarfadafan. (2024). Artificial Intelligence including Machine Learning and Deep Learning algorithms. *Advanced Tools for Studying Soil Erosion Processes*, 2024, 323-336. https://doi.org/10.1016/B978-0-443-22262-7.00020-5

[7] A. Ghosh, R. Maiti. (2021). Soil erosion susceptibility assessment using logistic regression, decision tree and random forest: study on the Mayurakshi river basin of Eastern India. *Environmental Earth Sciences*, 80, 328. https://doi.org/10.1007/s12665-021-09631-5

[8] R. Bag, I. Mondal, M. Dehbozorgi, S.P. Bank, D.N. Das, J. Bandyopadhyay, Q.B. Pham, A.M.F. Al-Quraishi, X.C. Nguyen. (2022). Modelling and mapping of soil erosion susceptibility using machine learning in a tropical hot sub-humid environment. *Journal of Cleaner Production*, 364, 132428. https://doi.org/10.1016/j.jclepro.2022.132428

[9] V. Gholami, H. Sahour, M.A.H. Amri. (2021). Soil erosion modeling using erosion pins and artificial neural networks. *Catena*, 196, 104902. https://doi.org/10.1016/j.catena.2020.104902

[10] H. Sahour, V. Gholami, M. Vazifedan, S. Saeedi. (2021). Machine learning applications for water-induced soil erosion modeling and mapping. *Soil and Tillage Research*, 211, 105032.https://doi.org/10.1016/j.still.2021.105032

[11] K.A. Nguyen, W. Chen, B.-S. Lin, U. Seeboonruang. (2021). Comparison of ensemble machine learning methods for soil erosion pin measurements. *ISPRS International Journal of Geo-Information*, 10(1), 42. https://doi.org/10.3390/ijgi10010042

[12] Y. Garosi, M. Sheklabadi, C. Conoscenti, H.R. Pourghasemi, K.V. Oost. (2019). Assessing the performance of GIS-based machine learning models with different accuracy measures for determining susceptibility to gully erosion. *Science of the Total Environment*, 664, 1117-1132.https://doi.org/10.1016/j.scitotenv.2019.02.093

[13] R.M.A. Ikram, M. Wang, H. Moayedi, A.A. Dehrashid, S. Gharibi, J.-C. Han. (2025). Application of smart technologies for predicting soil erosion patterns. *Scientific Reports*, 15, 26479. https://doi.org/10.1038/s41598-025-12125-0

[14] E. Mokhtari, M. Djeddou, I.A. Hameed, M. Shawaqfah. (2024). Advancing soil erosion prediction in Wadi Sahel-Soummam watershed Algeria: a comparative analysis of deep neural networks (DNN) and convolutional neural networks (CNN) models integrated with GIS. *BULLETIN OF THE SERBIAN GEOGRAPHICAL SOCIETY*, 104(1) 41-54. https://doi.org/10.2298/GSGD2401041M

[15] S. Senanayake, B. Pradhan, A. Alamri, H.-J. Park. (2022). A new application of deep neural network (LSTM) and RUSLE models in soil erosion prediction. *Science of the Total Environment*, 845, 157220. https://doi.org/10.1016/j.scitotenv.2022.157220

[16] T.V. Dinh, N.-D. Hoang, X.-L. Tran. (2021). Evaluation of different machine learning models for predicting soil erosion in tropical sloping lands of Northeast Vietnam. *Applied and Environmental Soil Science*, 2021, 6665485. https://doi.org/10.1155/2021/6665485

[17] J. Mallick, S. Alqadhi, S. Talukdar, M.N. Sarif,

T. Nasrin, H.G. Abdo. (2025). Evaluating soil erosion zones in the Kangsabati River basin using a stacking framework and SHAP model: a comparative study of machine learning approaches. *Environmental Sciences Europe*, 37, 34. https://doi.org/10.1186/s12302-025-01079-9

[18] X. Wang, D. Wang, T. Sun, J. Dong, L. Xu, W. Li, S. Li, P. Ran, J. Ao, Y. Zou, J. Wang, X. Zeng. (2023). Dual path attention network (DPANet) for intelligent identification of wenchuan landslides. *Remote Sensing*, 15(21), 5213. https://doi.org/10.3390/rs15215213

[19] W. Wei, J. Cao, N. Wang, Y. Qian. (2023). Multispectral remote sensing and DANet model improve the precision of urban park vegetation detection: an empirical study in Jinhai Park, Shanghai. *Frontiers in Ecology and Evolution*, 11, 1185911. https://doi.org/10.3389/fevo.2023.1185911

[20] C.C. Aggarwal. (2018). Neural networks and deep learning. *Springer Cham*. https://doi.org/10.1007/978-3-319-94463-0

[21] S. Wang, J. Cao, P.S. Yu. (2020). Deep learning for spatio-temporal data mining: A survey. *IEEE Transactions on Knowledge and Data Engineering*, 34(8), 3681-3700. DOI: 10.1109/TKDE.2020.3025580

[22] A. Graves. (2012). Long short-term memory, Supervised sequence labelling with recurrent neural networks. *Springer*, pp. 37-45. https://doi.org/10.1007/978-3-642-24797-2

[23] I.D. Mienye, T.G. Swart, G. Obaido. (2024). Recurrent neural networks: A comprehensive review of architectures, variants, and applications. *Information*, 15(9), 517. https://doi.org/10.3390/info15090517

[24] S. Yang, G. Berdine. (2017). The receiver operating characteristic (ROC) curve. *The Southwest Respiratory and Critical Care Chronicles*, 5(19), 34-36. https://doi.org/10.12746/swrccc.v5i19.391

[25] T.V. Phong, P.T. Trinh, B.N. Thanh, L.V. Hiep, B.T. Pham. (2025). Comparative analysis of machine learning and deep learning methods for coastal erosion susceptibility mapping. *Earth Science Informatics*, 18, 92. https://doi.org/10.1007/s12145-024-01587-x

[26] T.A. Tuan, P.V. Hong, T.T. Tam, N.T.A. Nguyet, N.V. Dung, P.T. Huy, T.V. Phong. (2025). Landslide susceptibility in Phuoc Son, Quang Nam: A deep learning approach. *Vietnam Journal of Earth Sciences*, 47(1), 39-57. https://doi.org/10.15625/2615-9783/21658

[27] A.P. Bradley. (1997). The use of the area under the ROC curve in the evaluation of machine learning algorithms. Pattern Recognition, 30(7), 1145-1159. https://doi.org/10.1016/S0031-3203(96)00142-2

[28] D.-H. Lee, Y.-T. Kim, S.-R. Lee. (2020). Shallow landslide susceptibility models based on artificial neural networks considering the factor selection method and various non-linear activation functions. *Remote Sensing*, 12(7), 1194. https://doi.org/10.3390/rs12071194

[29] C. Luu, D.D. Nguyen, M. Amiri, T.V. Phong, Q.D. Bui, I. Prakash, B.T. Pham. (2021). Flood susceptibility modeling using Radial Basis Function Classifier and Fisher's linear discriminant function. *Vietnam Journal of Earth Sciences*, 44(1), 55-72. https://doi.org/10.15625/2615-9783/16626

[30] R. Prăvălie, R. Costache. (2014). The analysis of the susceptibility of the flash-floods' genesis in the area of the hydrographical basin of Bâsca Chiojdului river. *Forum Geografic*, XIII(1), 39-49. doi:10.5775/fg.2067-4635.2014.071.i

[31] P.D. Rosa, A. Fredduzzi, C. Cencetti. (2019). Stream Power Determination in GIS: An Index to Evaluate the Most 'Sensitive'Points of a River. *Water*, 11(6), 1145. https://doi.org/10.3390/w11061145

[32] V.-H. Nhu, A. Mohammadi, H. Shahabi, B.B. Ahmad, N. Al-Ansari, A. Shirzadi, M. Geertsema, V.R. Kress, S. Karimzadeh, K.V. Kamran, W. Chen, H. Nguyen. (2020). Landslide detection and susceptibility modeling on cameron highlands (Malaysia): A

comparison between random forest, logistic regression and logistic model tree algorithms. *Forests*, 11(8), 830. https://doi.org/10.3390/f11080830

[33] P. Yariyan, S. Janizadeh, T.V. Phong, H.D. Nguyen, R. Costache, H.V. Le, B.T. Pham, B. Pradhan, J.P. Tiefenbacher. (2020). Improvement of best first decision trees using bagging and dagging ensembles for flood probability mapping. *Water Resources Management*, 34, 3037-3053. https://doi.org/10.1007/s11269-020-02603-7

[34] B.T. Pham, L.H. Trang, I. Prakash. (2025). Prediction of Optimum Water Content of soil using advanced machine learning methods: A comparative study of RF, SVM, and ANN models. *Vietnam Journal of Earth Sciences*, 47(3), 447-462. https://doi.org/10.15625/2615-9783/23484

[35] B.T. Pham, M. Amiri, M.D. Nguyen, T.Q. Ngo, K.T. Nguyen, H.T. Tran, H. Vu, B.T.Q. Anh, H. V. Le, I. Prakash. (2021). Estimation of shear strength parameters of soil using Optimized Inference Intelligence System. *Vietnam Journal of Earth Sciences*, 43(2), 189-198. https://doi.org/10.15625/2615-9783/15926

[36] Y. Nohara, K. Matsumoto, H. Soejima, N. Nakashima. (2019). Explanation of machine learning models using improved shapley additive explanation. *Proceedings of the 10th ACM international conference on bioinformatics, computational biology and health informatics*, pp. 546. https://doi.org/10.1145/3307339.3343255

[37] A. Chinnaraju. (2025). Explainable AI (XAI) for trustworthy and transparent decision-making: A theoretical framework for AI interpretability. *World Journal of Advanced Engineering Technology and Sciences*, 14(3), 170-207. https://doi.org/10.30574/wjaets.2025.14.3.0106

[38] M.R. Zafar, N. Khan. (2021). Deterministic local interpretable model-agnostic explanations for stable explainability. *Machine Learning and Knowledge Extraction,* 3(3), 525-541. https://doi.org/10.3390/make3030027

[39] A.J.A.S. Muhammad. (2024). Evaluation of Explainable AI Techniques for Interpreting Machine Learning Models.

[40] C.Q. Nguyen, T.T. Tran, T.T.T. Nguyen, T.H.T. Nguyen, T.S. Astarkhanova, L.V. Vu, K.T. Dau, H.N. Nguyen, G.H. Pham, D.D. Nguyen, I. Prakash; B.T. Pham. (2024). Mapping of soil erosion susceptibility using advanced machine learning models at Nghe An, Vietnam. *Journal of Hydroinformatics*, 26(1), 72-87. https://doi.org/10.2166/hydro.2023.327

[41] S. Senanayake, B. Pradhan, A. Huete, J. Brennan. (2020). A review on assessing and mapping soil erosion hazard using geo-informatics technology for farming system management. *Remote sensing*, 12(24), 4063. https://doi.org/10.3390/rs12244063

[42] Y. Darmawan, Munawar, D.A. Atmojo, H. Wahyujati, L. Nainggolan. (2023). Accuracy assessment of spatial interpolations methods using ArcGIS. *E3S Web of Conferences, 464, 09005. The 2nd International Conference on Disaster Mitigation and Management (2nd ICDMM 2023).* https://doi.org/10.1051/e3sconf/202346409005

[43] M. Michalopoulou, N. Depountis, K. Nikolakopoulos, V. Boumpoulis. (2022). The significance of digital elevation models in the calculation of LS factor and soil erosion. *Land*, 11(9), 1592. https://doi.org/10.3390/land11091592

[44] M. Li, X. Shi, Z. Shen, E. Yang, H. Bao, Y. Ni. (2019). Effect of hillslope aspect on landform characteristics and erosion rates. *Environmental Monitoring and Assessment*, 191, 598. https://doi.org/10.1007/s10661-019-7760-1

[45] Q. Liu, L. Chen, J. Li. (2001). Influences of slope gradient on soil erosion. *Applied Mathematics and Mechanics*, 22, 510-519. https://doi.org/10.1023/A:1016303213326

[46] D.H. Rieke-Zapp, M.A. Nearing. (2005). Slope

shape effects on erosion: a laboratory study. *Soil Science Society of America Journal*, 69(5), 1463-1471. doi:10.2136/sssaj2005.0015

[47] W. Zhongming, B.G. Lees, J. Feng, L. Wanning, S. Haijing. (2010). Stratified vegetation cover index: A new way to assess vegetation impact on soil erosion. *Catena*, 83(1), 87-93. https://doi.org/10.1016/j.catena.2010.07.006

[48] E. Babur, Ö.S. Uslu, M.L. Battaglia, A. Diatta, S. Fahad, R. Datta, M. Zafar-ul-Hye, G.S. Hussain, S. Danish. (2021). Studying soil erosion by evaluating changes in physico-chemical properties of soils under different land-use types. *Journal of the Saudi Society of Agricultural Sciences*, 20(3), 190-197. https://doi.org/10.1016/j.jssas.2021.01.005

[49] M. Singh, K. Hartsch. (2020). Basics of soil erosion, Watershed hydrology, management and modeling. *CRC Press*, pp. 38-61.

[50] A. Arabameri, J.P. Tiefenbacher, T. Blaschke, B. Pradhan, D.T. Bui. (2020). Morphometric analysis for soil erosion susceptibility mapping using novel gis-based ensemble model. *Remote Sensing*, 12(5), 874. https://doi.org/10.3390/rs12050874

[51] F. Bostanmaneshrad, S. Partani, R. Noori, H.-P. Nachtnebel, R. Berndtsson, J.F. Adamowski. (2018). Relationship between water quality and macro-scale parameters (land use, erosion, geology, and population density) in the Siminehrood River Basin. *Science of the Total Environment*, 639, 1588-1600. https://doi.org/10.1016/j.scitotenv.2018.05.244

[52] J. Benesty, J. Chen, Y. Huang, I. Cohen. (2009). Pearson correlation coefficient, Noise reduction in speech processing. Springer, pp. 1-4. https://doi.org/10.1007/978-3-642-00296-0_5

[53] C. Conoscenti, C.D. Maggio, E. Rotigliano. (2008). Soil erosion susceptibility assessment and validation using a geostatistical multivariate approach: a test in Southern Sicily. *Natural Hazards*, 46, 287-305.https://doi.org/10.1007/s11069-007-9188-0